MONITORING OF OSCILLATORY FAILURE CASES FOR THE REDUCTION OF STRUCTURAL LOADS IN AN AEROELASTIC AIRCRAFT

Helge Sachs, Udo B. Carl, Frank Thielecke
Hamburg University of Technology – Institute of Aircraft Systems Engineering

Keywords: *Oscillatory Failure Cases, Structural Loads, Monitoring System, Aeroservoelasticity*

Abstract

Allocated in the field of aeroservoelasticity, the present paper deals with flight control system failures and their impact on the aeroelastic structures of large transport aircraft (AC). Oscillatory Failure Cases (OFC), occurring as control surface (CS) oscillations, represent critical design cases and they must be detected by suitable monitoring systems. However, the threshold sensibility is limited by the avoidance of false alarms and unintended system shut-downs. Successfully reducing these thresholds without favoring accidental alarms allows to decrease the level of critical failure case loads. Finally, this holds the promise of structural weight savings. Compared to the reference detection thresholds of a given sensor-based OFC monitoring system (OFC-MS), an improved model-based monitoring approach is presented, which only depends on the on-board minimum sensor equipment. The results comprise an analysis of OFC failure causes and their effect on the flexible AC structures. Moreover, the conclusion is drawn to what extent the availability of an OFC-sensitive MS allows to alleviate such adverse effects. Validation is achieved using an actuation system test rig and an aeroelastic model of a representative civil large transport AC.

1 Introduction

Apart from safety and reliability the design of modern transport aeroplanes is increasingly characterized by economic efficiency, thus equivalent to the attempt to perpetually reduce the structural airframe weight for a given passenger capacity without compromising structural strength requirements. In civil aviation, particularly the long-stretched AIRBUS A340-600 or BOEING's B787 with its massive use of composite materials impressively demonstrate this ambition. This has led to increasingly longer, slenderer, and still lighter aircraft configurations. The described intent, however, goes to the detriment of aeroelastic stability because the modal spectral gap between weakly damped structural and flight mechanical modes decreases. With a growing aeroelastic responsiveness the flexible structures of an aeroplane are easily excited by either flight mechanical maneuvers, gusts, or unsteady air loads.

Numerous control strategies, as reviewed in [3, 1], harness the primary flight control (PFC) surfaces to actively damp structural vibrations with the major advantage to not need any further system equipment. The control algorithm is just implemented as add-on functionality in the flight control computers (FCC) of the digital flight control system, which is denoted by AIRBUS as Electronic Flight Control System (EFCS).

While the numerous advantages of the EFCS and the fly-by-wire (FbW) technology are well known, as introduced in civil aviation in the AIRBUS A320 in 1984, the higher overall system complexity has led to an increasing occurrence of *Oscillatory Failure Cases*. Among other reasons, hardly predictable interactions of hardware components (e.g. servo valve) and its assigned signal processing elements (e.g. current amplifier) rank among a long list of OFC causes, henceforth also called *OFC sources*. One illustrative example, having affected numerous airlines, is given later on.

Generally speaking, OFC trigger control surface oscillations, which may induce massive structural loads in e.g. wings, fuselage, and empennage due to the aeroservoelastic coupling of actuators and their respective CS. In a first consequence, OFC incidences are undesirable because they may lead to local structural overstress, thus considerably reducing an AC's fatigue life (fatigue damage accumulation). Yet, far more serious, CS oscillations do not only deteriorate the performance of the affected actuator, leaving the control system operative in degraded mode only, but – as a worst case scenario – undetected OFC could even entail an entire loss of flight mechanical control.

OFC-induced *failure case loads* become especially critical if the CS oscillation frequency matches the frequency of a dominant, weakly damped structural mode. Moreover, if the OFC frequency is adjacent to flight mechanical modes, this undermines the control authority of the superior flight laws, thus deteriorating the flight handling qualities. Complying with [8, 9], both scenarios have to be accounted for in dedicated loads analyses, as they represent design cases in the development process of fault-tolerant actuation systems and their integration in the surrounding flexible structure.

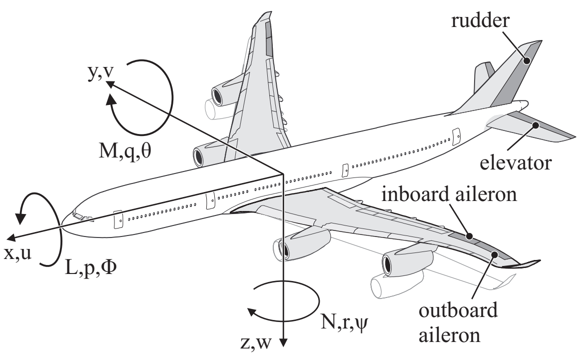

Fig. 1 Primary flight control surfaces of an aeroelastic aircraft

Fig. 1 illustrates the context of structure-system interactions of a highly flexible large transport aircraft, here an AIRBUS A340, which serves as exemplary AC in the subsequent investigations.

To counteract the aforementioned adverse effects immediate measures have to be taken to either prevent the occurrence of an OFC or, at least, best alleviate its impact on the structure. The chosen approach to both focus on OFC sources and suitable methods for a rapid and reliable OFC detection is described in [11]. However, given that the occurrence of OFC cannot be precluded by e.g. meeting stricter design requirements, the only solution to the problem is an OFC-sensitive monitoring system.

Various patents [14, 5, 6] related to the monitoring of OFC are clearly sensor-based and partly depend on sensors (e.g. servo valve spool position transducer) that not all PFC actuators are equipped with. Therefore, the given paper proposes a minimum sensor-dependant model-based OFC-MS. Apart from minimum required detection thresholds the MS must proof to be robust to unmodeled disturbances and parametric uncertainties to obviate false alarms and unintended system shut-downs. The observer-based monitoring system is developed in a simulation model environment and subsequently tested on an A340 actuation test rig to determine the specific MS performance, i.e. the minimum obtainable detection thresholds at zero false alarm rate. Finally, the OFC-MS thresholds are used to calculate failure case loads with the aforementioned aeroelastic A340 loads model, thus validating the OFC-MS performance in terms of *allowable angles*.

The paper follows the subsequent structure: Section 2 briefly describes an exemplary PFC actuation system with corresponding test rig for the experimental investigations. Section 3 illustrates the variety of OFC sources taken into account and gives an example of an OFC in-service incident, thus revealing the complexity of the problem and how difficult it can be to preclude any imaginable fault scenario despite taking all mandatory precautions. Therefore, a model-based MS is proposed, which is dedicated to the detection of

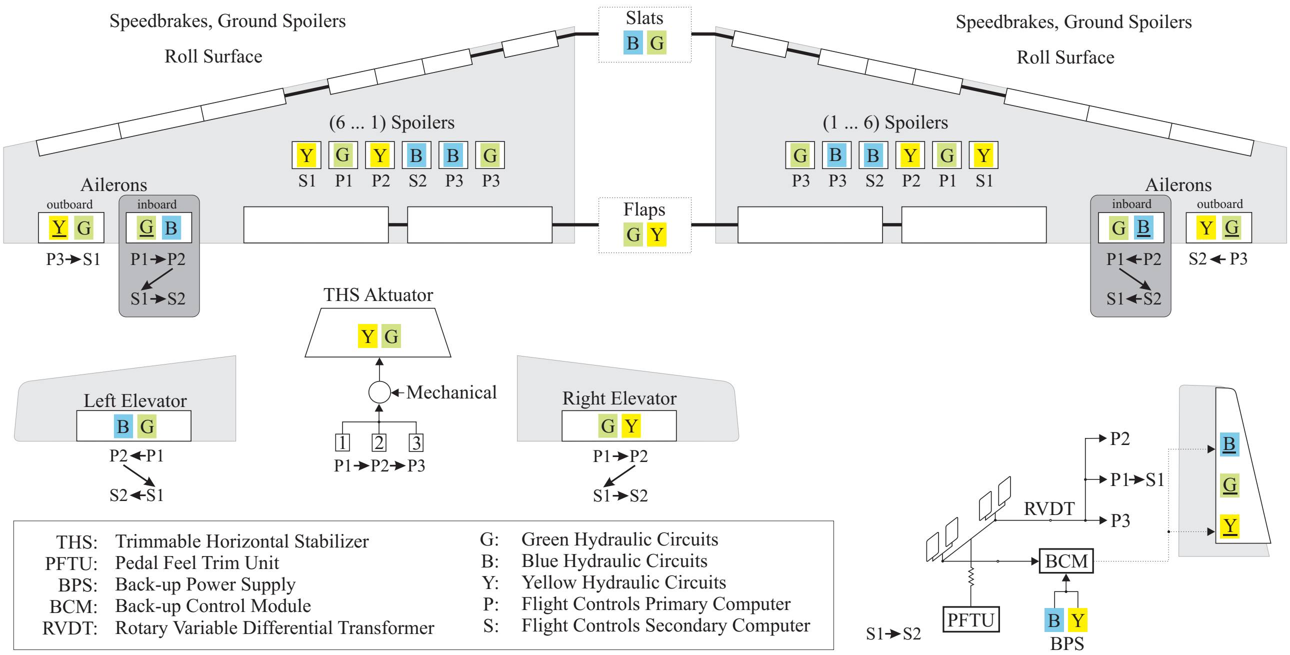

Fig. 2 Flight control system architecture of an A340 ENHANCED with FbW rudder control

OFC. This OFC-MS is tested and the results are presented in Section 4. The obtainable monitoring performances are validated applying the suggested method to a representative large transport AC, here an AIRBUS A340. Concluding remarks finalize the paper.

2 System Description and Modeling

The approach to the development of an OFC-MS starts with a detailed modeling of a representative actuation system, here an A340 inboard aileron actuation system. Model validation and system parameter identification are achieved by means of test rig measurements. The finally obtained non-linear and time-discrete actuation system modeling is used as basis for the subsequent modeling of the remaining primary actuation systems, i.e. outboard ailerons, elevators, and rudder. The different actuation system models are coupled to the aeroelastic AC loads model using specific attachment stiffness and damping coefficients for each control surface. Finally, the model-based monitorings are designed and adapted to each actuation system.

2.1 Primary Flight Control System

The different actuation systems to be investigated belong to the latest digital fly-by-wire primary flight control system (PFCS) of the A340 ENHANCED. Fig. 2 depicts the exemplary flight control system architecture. Three hydraulic systems supply the primary and secondary flight controls. Each control surface is operated by its dedicated FCC without any further mechanical back-up system. The EFCS is composed of five FCC (three primary P1, P2, P3 and two secondary S1, S2). Both replicated hardware and software with dissimilarity in command and monitor channels guarantee quintuple redundancy. The FCC operate in parallel to minimize delay times in case of switching processes after single or multiple failures. Below each primary control surface the FCC hierarchies are shown.

2.2 Actuation System Modeling

The ailerons are used for roll control, maneuver load alleviation, and aileron droop, the latter to support the high lift devices during landing. Fig. 3 illustrates the duplex configuration of this actuation system with two position-controlled electro-hydraulic servo actuators (EHSA). Conventionally, one EHSA is active and controls the CS deflection, while the stand-by actuator is switched to the damping mode through the mode selector valve (MSV), thereby contributing to the damping characteristics of the actuation system. Moreover, the passive actuator prevents the occurrence of flutter effects in case of multiple hydraulic or electrical failures.

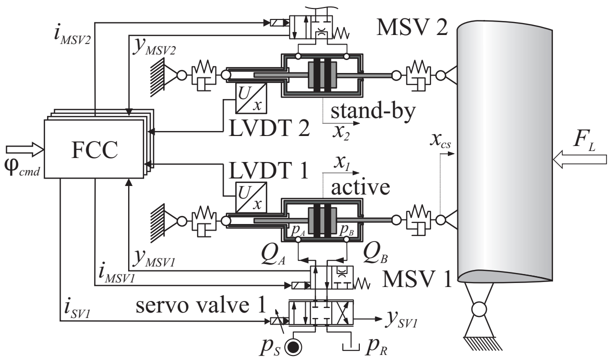

Fig. 3 Duplex actuation control system

The non-linear and time-discrete modeling approach is presented in detail in [12]. Basically, the non-linear EHSA system modeling takes into account the servo valve dynamics with amplifier current i_{SV} and spool displacement y_{SV}, a mode selector valve with solenoid current i_{MSV}, the chamber flows $Q_{A,B}$ due to pressure change $\mathrm{d}p_{A,B}/\mathrm{d}t$, and the piston position x. System inputs are the commanded deflection φ_{cmd} and external forces F_L, resulting from the reaction forces of an unsteady air flow on the deployed surface. The control loop is closed with the feedback position signal x, which is on the test rig measured with a linear variable differential transformer (LVDT).

Considering Section 3, a number of potential OFC causes originate from erroneous signal and data processing. Fig. 5 indicates some of the components in the digital signal processing chain that proved to favor the emergence of OFC. The corresponding results are presented in [11, 12]. To investigate such signal processing fault scenarios in a model environment the originally non-linear, quasi-continuous models were refined, thus yielding non-linear time-discrete actuator models. These models were used to analyze the dependency of closed-loop stability margins on a set of selected system parameters, such as delay and sampling times, or the resolution of the analog/digital converters. As indicated, the investigations are limited to the actuator servo loop.

2.3 Experimental Test Rig

Both system identification and the investigation of some OFC failure scenarios is accomplished using an experimental test rig that was set up at the INSTITUTE OF AIRCRAFT SYSTEMS ENGINEERING. Two original A340 inboard aileron actuators are mechanically coupled through a shaft to two inertia disks, which represent the exact moment of inertia of the aileron. For the purpose of load simulations another EHSA is attached to the shaft in opposite direction of the actuation system. The *hardware-in-the-loop* (HIL) test rig is embedded in a Matlab/Simulink^{TM} real-time simulation environment. Thus, it can be used to demonstrate the impact of hardware-induced OFC on the flexible structures of the aeroelastic AC model. This allows to determine the OFC-induced failure case loads. Fig. 4 illustrates the aeroservoelastic testing environment. The target computer controls the test rig in real-time according to the measurement sequence defined on the host computer. Optionally, the test rig replaces one of the aileron actuation system models for the investigation of realistic fault scenarios. All further tasks are performed on the host computer, i.e. calculating the failure case loads, analyzing the OFC causes, and monitoring the different actuation systems.

3 Investigation of OFC Causes

The different causes for the emergence of OFC are investigated for two reasons. First of all, a true understanding of what may favor or contribute to control-loop instabilities evolving into CS oscillations allows to draw conclusions and derive design recommendations for the development process of fault-tolerant flight actuation

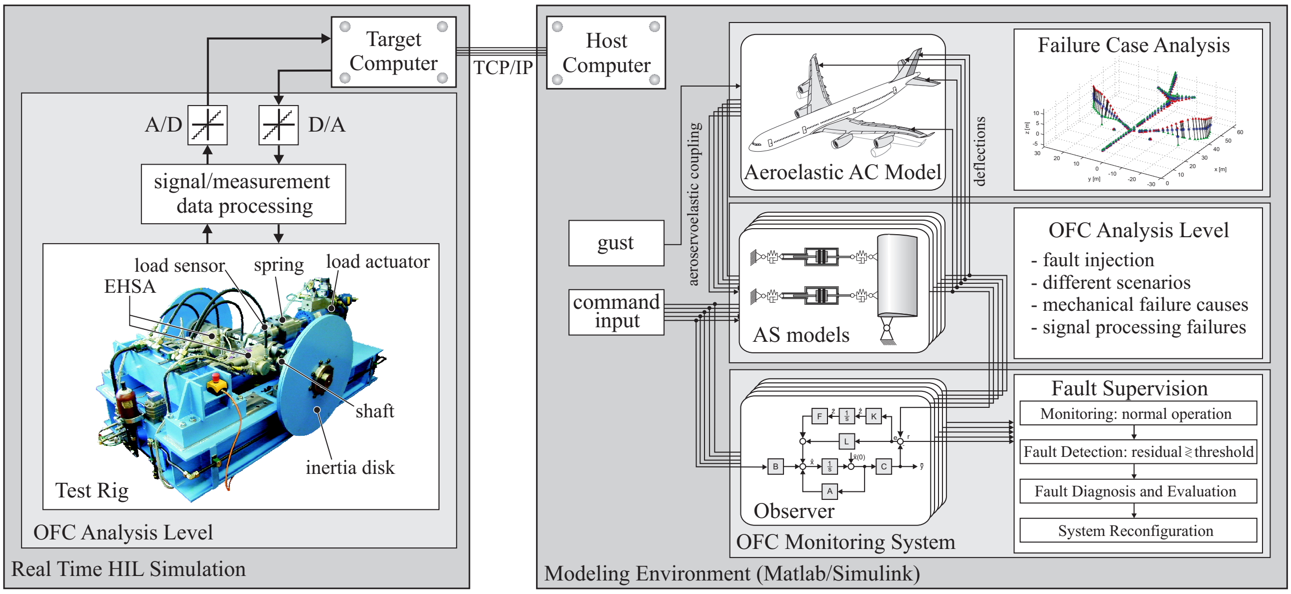

Fig. 4 Simulation and testing environment

systems. Moreover, good knowledge about OFC sources and their location in the signal processing chain, as indicated in Fig. 5, is necessary for the design of an OFC-sensitive MS. Depending on the desired threshold sensibilities of the OFC-MS or another possible requirement to not only detect the OFC but also identify its location, the minimum number of sensors has to be determined for the fault diagnosis process. While additional sensors may improve the diagnosability of the system, this does not necessarily have to make sense keeping in mind the increasing overall system complexity; particularly, because sensors must be testable or, even better, redundant. Thus, a thorough investigation of the potential OFC sources is a prerequisite for the design of the OFC-MS, presented in Section 4.

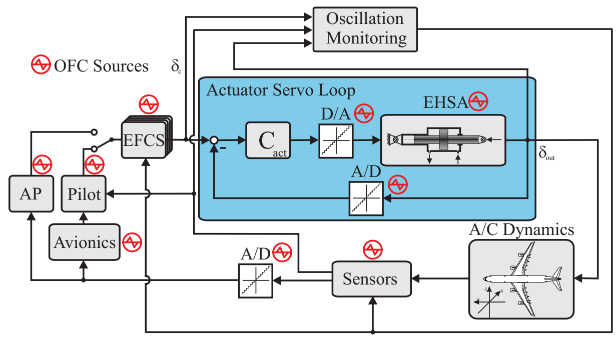

Fig. 5 Potential OFC sources in the signal processing chain of a PFC actuation system

3.1 Investigational Scope

OFC may originate from an immense variety of failure causes. Neither open literature research offers valuable clues to the question where and why OFC occur, nor corresponding failure mode and effects analyses (FMEA) of all relevant components were available. The approach to the investigation of OFC sources is mainly based on a number of technical discussions and internal documents of either AIRBUS, as aircraft manufacturer, LIEBHERR AEROSPACE LINDENBERG GMBH, a major supplier of flight control (actuation) systems, or LUFTHANSA TECHNIK AG (LHT), one of the world market leaders in the AC maintenance, repair and overhaul (MRO) business. The following overview in Fig. 6 summarizes the different classes of potential OFC sources. Basically, the failure hypotheses taken into consideration are classified into three major categories. In some cases, however, the failure causes could also be assigned to more then just one category. Therefore, a forth subsection is added, containing all OFC sources that could not be clearly added to any of the three aforementioned classes. An example of mechanical fault causes, i.e. the fracture of the servo valve feedback spring, is discussed in [11]. The focus will be here on signal processing failures, which may evolve into an OFC.

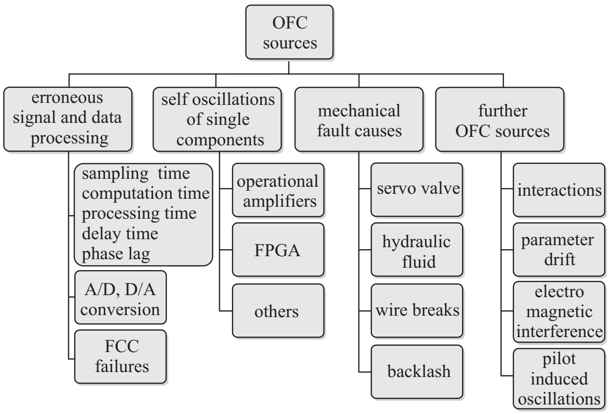

Fig. 6 Overview of the different potential OFC sources

3.2 Signal Processing Failures

Digital flight control systems have specific maximum allowed *sampling times*, *computation times*, *overall processing times*, and *delays*. These time intervals, however, are subject to variations and cannot be exactly guaranteed. Therefore, the time intervals are limited to specific maximum values complying with the required stability margins. The control system is designed such as to cope with these uncertainties so that the system dynamics must not be destabilized as long as the specified time intervals are within the required tolerance range.

In the following, the dependency of the closed-loop stability of the actuator servo loop on three parameters is presented. The parameters (with given nominal values) considered to be most relevant in the framework of OFC-related signal processing failures are

- the delay time with $t_{d,nom} = 2$ ms,
- the sampling time with $t_{s,nom} = 10$ ms,
- and the resolution of the analog/digital unit (ADU) with $n_{nom} = 16$ bits.

Considering *Shannon*'s sampling theorem [13] for the given sampling time $t_{s,nom} = 10$ ms frequencies up to $f_{max,shannon} = 50$ Hz in the analog signal could be theoretically reconstructed from the digital signal. This is of course not necessary because the highest required deflection rates for the actuation system are in the range of a few hertz. Higher frequencies, which might be fed into the actuator servo loop by the EFCS, are even compensated for by rate limiters. Moreover, the highest sampling frequency to be still reconstructed according to Shannon is multiplied by a safety factor to further reduce the risk of aliasing effects. For the aforementioned investigational purpose to analyze system instabilities, however, the Shannon theorem is not sufficient.

Thus, three different analytic criterions were used which led to results with good accordance. The methods were as follows:

- the *Nyquist stability criterion* to test the closed-loop system stability by analyzing the open-loop Nyquist plot in the frequency domain,
- the *harmonic balance analysis* to examine non-linear characteristic ADU curves with corresponding failures types (e.g. bit degradation, non-linearities, offset) in the frequency domain,
- the *overshoot criterion* concluding from step responses in the time domain on the closed-loop stability.

The latter is briefly presented herein. The approach determines the maximum overshoot after a step response in a distinct time interval, here the last 10 percent of the simulation time. The following parameter intervals are considered

$$\begin{aligned} n &= [8\ldots 16 \text{ bits}] \quad , \\ t_s &= [10\ldots 80 \text{ ms}] \quad , \\ t_d &= [2\ldots 30 \text{ ms}] \quad . \end{aligned} \tag{1}$$

The subsequent Fig. 7 illustrates the comparable results obtained on the experimental test rig on the left hand side and with the simulation model on the right side.

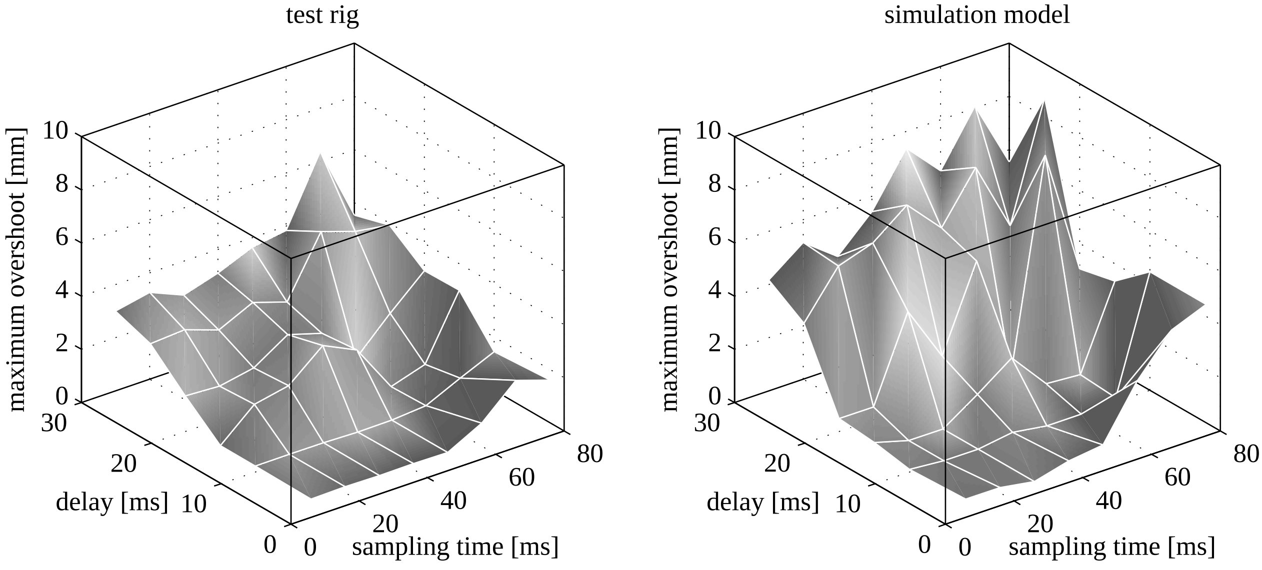

Fig. 7 Maximum overshoot after a step response ($x_{cmd} = 1$ mm) in time interval $t = 2.7\ldots3$ s ($n = 8$ bits)

Generally, it can be stated that both test rig and model reveal increasing overshoots for large deviations from the nominal parameters. Although the model reacts with higher sensitivity both results lead to the identical parameter regions for a stable system. The frequency domain analyses with the Nyquist and harmonic balance criterions confirmed the obtained parameter regions ($n \geq 8$ bits, $t_s \leq 40$ ms, $t_d \leq 10$ ms).

3.3 OFC In-service Incident

The following example illustrates the complexity of the OFC problem and the difficulty to preclude any imaginable fault scenario despite complying with the system safety requirements.

Each wing of the Airbus A330/A340 is equipped with six spoilers that are all used for lift damping, partly as speed brakes, or they are integrated in the roll control function. Although the spoiler actuators had to undergo vibration tests to identify their resonance spectrum in three orthogonal axes, as specified in RTCA-DO 160 [10], resonance in the first stage of the electro-hydraulic servo valve (EHSV) caused an operational loss of the affected actuator. The actuators were originally equipped with two-stage servo valves with an electro-mechanical governor (torque motor), a hydraulic amplifier (deflector jet type) as pilot stage (first), and the hydraulically controlled spool in the main stage (second) connected to the torque motor via a mechanical feedback. Fig. 8 shows the spoiler positions on the wing with corresponding spoiler actuators and a cross-section diagram of the two-stage servo valve.

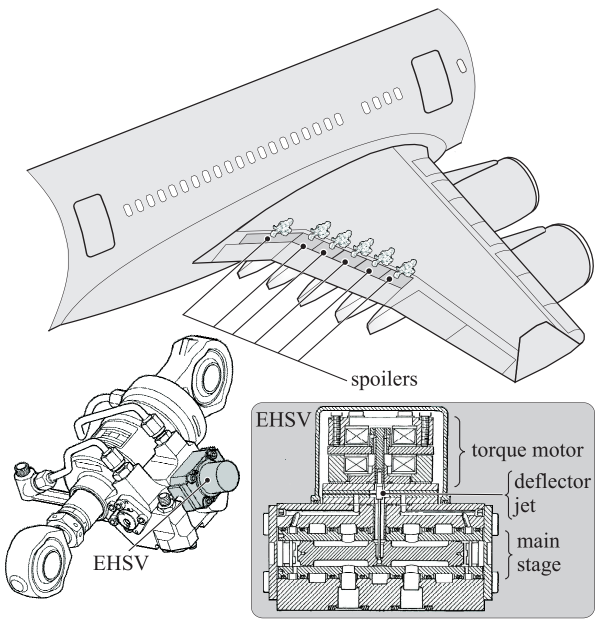

Fig. 8 A340 spoiler actuation system

Once the actuators were installed wing vibrations induced by unsteady air loads excited the

– as it turned out – insufficiently damped spool, thus causing a back electro-magnetic force in the torque motor, which started to oscillate at its natural frequency around 700 Hz. The failure could be detected by the servo valve monitoring and the actuators were passivated before sustaining serious damage.

The problem was solved by using another servo valve type with different working principle as pilot stage and higher damping characteristics, switching from the deflector jet to the jet pipe principle.

4 OFC Monitoring

Considering the historical background of failure detection and diagnosis systems, a transition from exclusively sensor-based to sensor/model-based concepts is currently taking place in all sorts of high-technology products. Conventionally, monitoring concepts for complex control systems, such as in aerospace applications, check if single measured variables exceed specific limit thresholds; if so the MS triggers an alarm and initiates system reconfiguration. To give an example, the occurrence of a powered runaway in PFC actuation systems is normally monitored by comparing commanded and measured actuator position signals. In its most straightforward realization the runaway MS supervises if the control deviation exceeds a fixed threshold for the duration of a specific time interval. This defines a failure symptom, which releases the switching from the faulty to the stand-by actuator.

Yet, notwithstanding the advantages of sensor-based monitoring systems, model-based diagnosis holds the promise to harness the (hidden) information of both measurable and non-measurable processes. The basic idea is to simultaneously improve a system's diagnosability without using additional sensors. While the number of hurdles to overcome considering all sorts of certification issues is immense, model-based diagnosis finds its way into the supervision of even safety-critical systems [4]. The potential of model-based diagnosis in complex aviation control systems could be successfully demonstrated in [7], proposing a model-based electronic torque limitation concept for the detection of hard and soft jams in high-lift actuation systems.

The OFC monitoring system to be presented in the following uses a model-based approach. Depending only on the actuator piston LVDT signal as input, the concept allows for considerably reduced detection thresholds compared to the reference thresholds of the given A340 OFC-MS. Initially, different model-based detection methods were developed in the simulation model environment of the described inboard aileron actuation system. The three investigated methods were a *Luenberger State Observer* [11], a *Disturbance Observer* [12], and a Kalman filter based approach (*Unscented Kalman Filter*). The method to be chosen has to comply with the following set of requirements:

- minimum achievable detection thresholds, which determine the *monitoring performance*,
- highest possible detection speed,
- minimum false alarm rate (robustness to disturbances like external loads, measurement noise) for highly dynamic system excitation,
- dependence on minimum sensor equipment,
- implementability in the real-time HIL testing environment (online detection).

The Disturbance Observer turned out to be the most promising and reliable approach. Considering its initial presentation in [12], the method was refined. As the method was undergoing an elaborate test case series, the adaptive threshold computation was improved, thus making the method less prone to false alarms. Moreover, the actual failure detection process was extended by adding a procedure that initializes system reconfiguration by passivating the faulty actuator and switching to the stand-by actuator.

Fig. 9 shows the structure of the Disturbance Observer, which uses the inputs and outputs of

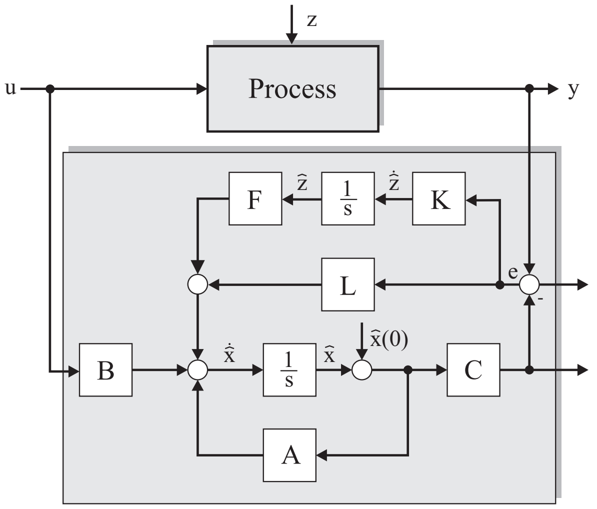

Fig. 9 Disturbance Observer

the actual system to reconstruct the actuator position signal. The observer is restricted to the linearized equation of motion of the active actuator, which is embedded in a non-linear representation of the actuation system. The obtained residual

$$\mathbf{r} \;=\; \mathbf{y}-\hat{\mathbf{y}} \tag{2}$$

is evaluated using an adaptive threshold functional to determine whether the original system contains a fault. The state space representation of the disturbance observer is given as

$$\begin{aligned}
\dot{\hat{\mathbf{x}}} &= (\mathbf{A}-\mathbf{LC})\,\hat{\mathbf{x}}+\mathbf{Bu}+\mathbf{Ly}+\mathbf{F}\hat{\mathbf{z}} && (3)\\
\dot{\hat{\mathbf{z}}} &= \mathbf{Ke}=\mathbf{K}\,(\mathbf{y}-\hat{\mathbf{y}}) && (4)\\
\hat{\mathbf{y}} &= \mathbf{C}\hat{\mathbf{x}} \quad , && (5)
\end{aligned}$$

where **L** is the observer feedback matrix. The pole placement of the observer eigenvalues $\lambda_{i,obs}$ with $i \in (1,2)$ is a tradeoff between high desired detection speeds and minimum sensitivity to measurement noise. The observer eigenvalues are calculated with the eigenvalues of the linearized plant $\lambda_{i,sys}$ as follows

$$\lambda_{i,obs} = k\cdot\Re\left\{\lambda_{i,sys}\right\} + j\cdot\frac{\Im\left\{\lambda_{i,sys}\right\}}{k} \quad . \tag{6}$$

The variable k is empirically determined. To best account for unmodeled additive and multiplicative faults, such as parametric system uncertainties and measurement noise, the observer output error **e** is fed back via the matrix **K**, an integrator, and the matrix **F**. Therein the integrator compensates for remaining steady-state errors.

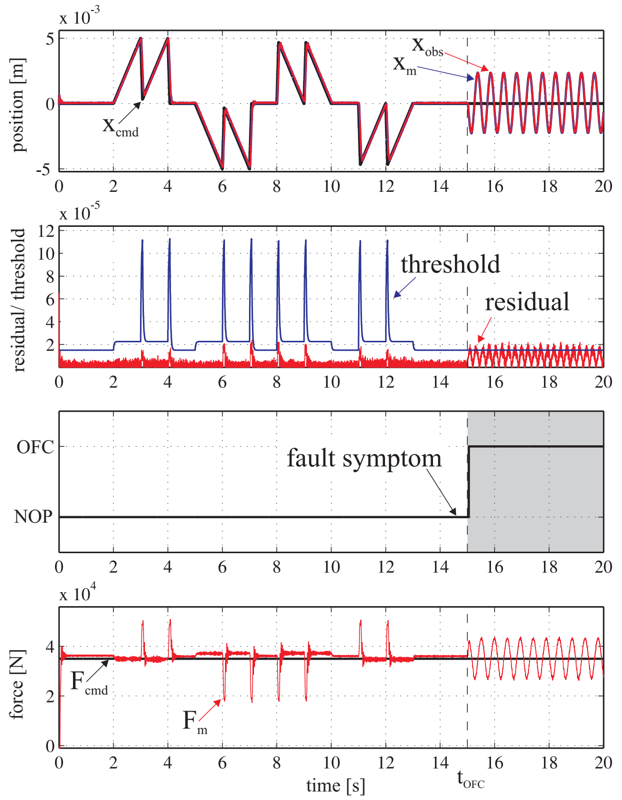

Fig. 10 OFC-MS robustness test in the presence of simulated unsteady air loads

Fig. 10 shows the detection of a sinusoidal OFC occurring at $t_{OFC} = 15$ s. To show that the observer-based MS reliably detects OFC without triggering false alarms the commanded control inputs are highly dynamic. Simultaneously, the actuation system encounters disturbance forces acting as simulated air loads on the piston. The measurement plots in Fig. 10 consecutively show

- the commanded, measured and observed positions (x_{cmd}, x_m, x_{obs}),
- the residual and corresponding adaptive threshold,
- the evaluated residuals as fault symptom (NOP for normal operation or OFC),

- the commanded and measured disturbance force (F_{cmd}, F_m).

Notwithstanding the highly dynamic position commands or the inevitable and realistic load peaks when the actuator rapidly moves in its opposite direction, the MS does not erroneously release a false alarm.

According to the aforementioned requirements a suitable monitoring system does not only have to detect the OFC but also maintain the system's operability in a failure event. Therefore, this ability was implemented. The following measurement plots in Fig. 11 illustrate the process of system reconfiguration initiated by the model-based OFC-MS after an OFC occurring at $t_{OFC} = 10$ s.

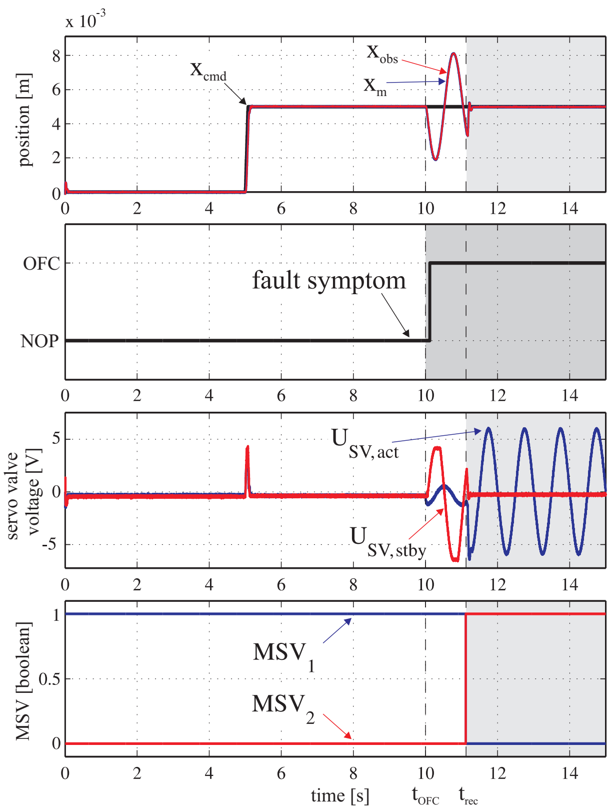

Fig. 11 OFC-MS initiates system reconfiguration

In addition to the position signal and the fault symptom the lower two plots show the servo valve voltages and MSV switching of the two EHSA. After the formerly passivated stand-by actuator is activated the faulty actuator is passivated and its respective servo valve continues to oscillate. The confirmation time between the failure detection and the successful system reconfiguration was deliberately set to $t_{conf} = 1$ s to better visualize the reconfiguration process. In fact t_{conf} can be limited to a single sampling time interval of just

$$t_{conf,min} = \Delta t_{s,nom} = 10 \text{ ms} \quad . \qquad (7)$$

Finally, the overall monitoring performance of the observer-based detection method is presented in terms of minimum achievable, frequency-dependent detection thresholds. As the OFC-MS was validated by means of an aileron actuation system, Fig. 12 illustrates the minimum detection threshold $\xi_{det,obs}$, which is here normalized to the required minimum detection threshold $\xi_{det,req}$ of the A340 reference OFC-MS.

The elaborate test case series covers the relevant frequency range from 0.1 to 10 Hz. It also accounts for different OFC signal signatures (triangular, sinusoidal) and different commanded step heights x_{cmd}, indicated as solid (1 mm) and dashed lines (30 mm). The different step heights serve the purpose to test the observer's sensibility to high deviations from its operating point.

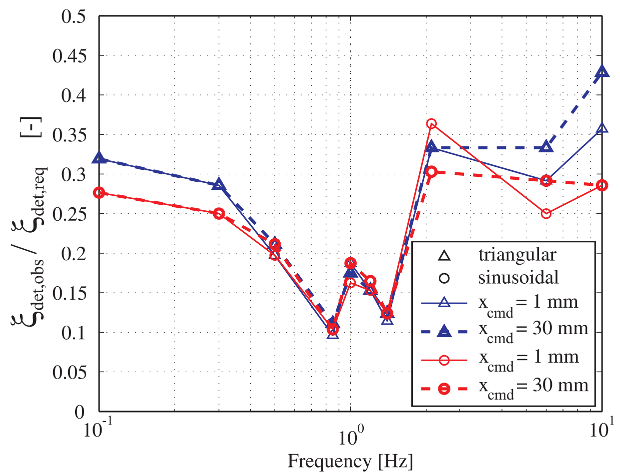

Fig. 12 MS performance as minimum observer-based OFC detection threshold compared to A340 reference OFC-MS

Considering the reference OFC-MS, the minimum achievable detection thresholds could be considerably reduced with the observer-based failure detection method.

5 Reduction of Failure Case Loads

Recalling the actual goal that the availability of an improved OFC monitoring system shall serve the purpose to reduce the failure case loads level, this section reviews in how far the proposed observer-based OFC-MS complies with this intent. The MS validity assessment is based on the so-called *allowable angles criterion* [2]. It is used by AIRBUS in the design and certification process of flight control systems and their integration in the structure, thus in the field of structure-system interactions [9]. The allowable angles are the maximum oscillatory CS deflection amplitudes, which cause failure case loads that do not exceed the limit loads $L_{L,i}(\omega)$. The variable i defines the overall number of load cases. These load cases comprise the OFC-induced forces, bending and torsional moments, also denoted by load interesting quantities (LIQ), at various cut sections in all relevant airframe structures. Moreover, the LIQ are determined for several critical points in the flight envelope (flight altitude and Mach number) and various AC mass cases (variable load distribution due to fuel consumption).

The frequency-dependent transfer functions

$$|H_{\varphi L_i}(\omega)| = \frac{|L_i(\omega)|}{|\delta_{unit}(\omega)|} \qquad (8)$$

are calculated with the flexible AC loads model where the CS deflection amplitude is set to $|\delta_{unit}| = 1°$. Thus, the obtained unit loads for harmonic oscillatory unit deflections are defined as $L_i(\omega)$. According to the aeroelastic responsiveness the transfer functions $|H_{\varphi L_i}(\omega)|$ show several peaks at distinct frequencies which characterize the modal eigenfrequencies of the flexible AC structure.

With the limits loads $L_{L,i}(\omega)$, as obtained in static loads calculations, the maximum allowed CS deflection angles can be calculated for each LIQ in each cut section as

$$\varphi_{i,max}(\omega) = \frac{L_{L,i}}{|H_{\varphi L_i}(\omega)|} \quad . \qquad (9)$$

The allowable angles curve is finally determined in a minimum search as follows

$$\varphi^{AA}(\omega) = \min_i \{\varphi_{i,max}(\omega)\} \quad . \qquad (10)$$

Thus, if the structure is excited by CS oscillations with $\varphi^{AA}(\omega)$ the design limit load envelope is just covered but never exceeded. With respect to an OFC-MS performance assessment it first has to be guaranteed that the allowable angles curves do not fall below the MS threshold. Fig. 13 illustrates for the A340 inboard aileron that this already applies to the reference OFC monitoring system. However, the observer-based minimum detection thresholds (red curve) show a considerable reduction for the entire frequency range, which holds the promise of weight savings in the design and certification process.

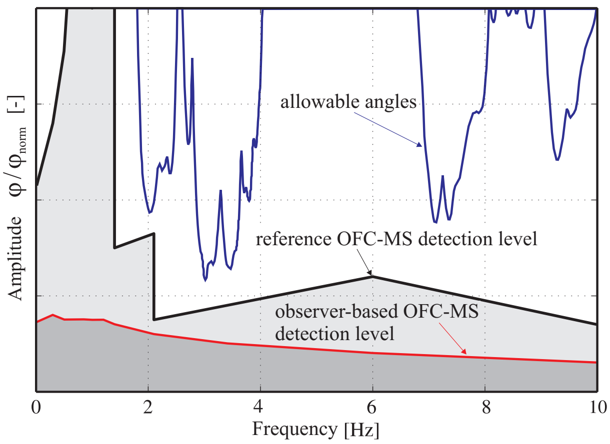

Fig. 13 Allowable angles for the inboard aileron actuation system and comparison of different minimum detection thresholds

6 Conclusion

Given that the occurrence of oscillatory failure cases in flight control systems cannot be absolutely precluded by meeting stricter design requirements, modern civil aircraft must be equipped with dedicated monitoring devices. OFC do not only deteriorate the flight handling qualities. In a worst case scenario they may even lead to a loss of control if they remained undetected. Less severe but also undesirable, OFC cause massive structural loads, related to as failure case loads, and as a final consequence reduce an AC's fatigue life. Considering a representative A340 actuation control system, the system model and corresponding hardware-in-the-loop test rig are presented. Both the actuation system models and the test rig are used to investigate OFC sources, which is necessary for the design of an OFC-sensitive MS. An observer-based OFC-MS is proposed and tested both in terms of robustness requirements and its sensibility to release false alarms. Although the model-based failure detection method only depends on the on-board sensor equipment, the approach allows for reduced detection thresholds when comparing it to the given A340 OFC reference MS. The achievable monitoring performance is presented in terms of minimum detection thresholds. Finally, evidence is given that the proposed OFC-MS allows to both alleviate the impact of OFC-induced loads and reduce the failure case loads level. This is demonstrated by means of the allowable angles criterion.

Acknowledgements

The authors thank AIRBUS DEUTSCHLAND GMBH for promoting the investigations within the framework of the research project Multi Objective Dynamic Aircraft Synthesis (MODYAS). The technical support of LIEBHERR AEROSPACE LINDENBERG GMBH and LUFTHANSA TECHNIK AG widely contributed to the progress of the research activities.

References

[1] ENZINGER, M.F.: *A Modal Control Approach Based on a Minimum-Order Dynamic Feedback*. Doctoral Thesis, FernUniversität Hagen. Scientific series: Aircraft Systems Engineering. Aachen, Germany : Shaker Verlag, 2005.

[2] GIESSELER, H.-G. ; BESCH, H.-M.: The Oscillatory Failure Identification System OFIS. In: *36th AIAAS/ASME/ASCE/AHS/ASC Structures, AIAA-95-1112-CP*. Los Angeles, USA, 1995.

[3] GOJNY, M.H.: *Systemtechnische Untersuchungen zur aktiven Regelung aeroelastischer Schwingungen bei Transportflugzeugen*. Doctoral Thesis, Hamburg University of Technology. Scientific series: Aircraft Systems Engineering. Aachen, Germany : Shaker Verlag, 2005.

[4] ISERMANN, R.: *Fault Diagnosis Systems. An Introduction from Fault Detection to Fault Tolerance*. Berlin : Springer, 2005.

[5] LE, L.T.: *Oscillatory Failure Monitor*. The Boeing Company. United States Patent. Seattle, Washington, USA, 1989.

[6] MANUBHAI, C.: *Oscillatory Servo-Valve Monitor*. Boeing Commercial Airplane Group. United States Patent. Seattle, Washington, USA, 1994.

[7] NEUMANN, U. ; CARL, U.: Development and Experimental Validation of Model Based Electronic Torque Limitation for High Lift Systems. In: *Proceedings of the 1st International Workshop on Aircraft System Technologies*. Hamburg, Germany, 2007.

[8] JOINT AVIATION AUTHORITIES – JAA (Ed.): *Joint Aviation Requirements, JAR–25: Large Aeroplanes*. Cheltonham, England : Westwood Digital Limited, 1997.

[9] JOINT AVIATION AUTHORITIES – JAA (Ed.): *Notice of Proposed Amendment (NPA), NPA 25C-199, Interaction of Systems and Structures*. Cheltonham, England : Westwood Digital Limited, 2004.

[10] RADIO TECHNICAL COMMISSION FOR AERONAUTICS – RTCA (Ed.): *Environmental Conditions and Test Procedures for Airborne Equipment*. Washington D.C., USA, 2007.

[11] SACHS, H.; CARL, U. ; THIELECKE, F.: An Approach to the Investigation of Oscillatory Failure Cases in Electro-Hydraulic Actuation Systems. In: *International Conference on Recent Advances in Aerospace Aerospace Actuation Systems and Components*. Toulouse, France, 2007.

[12] SACHS, H.; CARL, U. ; THIELECKE, F.: Impact of Oscillatory Failure Cases in Electro-Hydraulic Actuation Systems on an Aeroelastic

Aircraft. In: *2007 SAE AeroTech Congress & Exhibition*. Los Angeles, USA, 2007.

[13] SHANNON, C.E.: Communication in the Presence of Noise. In: *Proc. Institute of Radio Engineers*, 1949.

[14] SKONIECZNY, R.D.: *Oscillatory Failure Monitor*. United Technologies Corporation. United States Patent. Hartford, Connecticut, USA, 1986.

Copyright Statement